Fabrication and performance evaluation of tannin iron complex (TA-Fe^{III}/PES) UF membrane in treatment of BTEX wastewater

Takalani Makhani[1], Olawumi O Sadare[1], Stephan Wagenaar[2], Kapil Moothi[1], Richard M Moutloali[2] and Michael O Daramola[3]

[1]*Department of Chemical Engineering, Faculty of Engineering and the Built Environment, Doornfontein Campus, University of Johannesburg, PO Box 17011, Johannesburg 2028, South Africa*

[2]*Department of Chemical Sciences, University of Johannesburg, PO Box 17011, Doornfontein 2028, Johannesburg, South Africa*

[3]*Department of Chemical Engineering, Faculty of Engineering, Built Environment and Information Technology, University of Pretoria, Hatfield 0028, Pretoria, South Africa*

Oil exploration generates produced water that is characterized as hazardous and toxic waste. Produced water contains a mixture of various pollutants, including monoaromatic hydrocarbons BTEX (benzene, toluene, ethylbenzene, and xylene), compounds that are carcinogenic even in small concentrations. In this study, tannin iron complex (TA-Fe^{III}), blended into polyethersulfone (PES) membrane was evaluated for the treatment of BTEX-containing wastewater. The membranes were fabricated using the non-solvent induced phase separation (NIPS) method and loading of the TA-Fe^{III} complex on the membranes varied from 0–0.9 wt%. The fabricated membranes were characterized using various techniques such as scanning electron microscopy (SEM), water contact angle (WCA), Fourier transform infrared (FTIR) spectroscopy, and atomic force microscopy (AFM) to check the surface morphology, hydrophilicity, surface functionality and surface roughness of the fabricated membranes, respectively. The TA-Fe^{III} modified membranes showed increased pure water flux from 100 (PES 0) to ~150 (PES 0.9) L/(m^2·h) at 100 kPa. The performance of the fabricated membranes was tested using 70 mg/L synthetic BTEX solution. Overall BTEX rejection > 70% was achieved at increasing TA-Fe^{III} loadings compared to BTEX rejection < 65% for the pure PES membrane. Rejection of the BTEX compounds was mainly through the size exclusion mechanism. These modified TA-Fe^{III}/PES UF membranes proved to be effective in the treatment of BTEX-containing water, and also have the potential to be applied in oily wastewater treatment.

INTRODUCTION

Clean water is essential for the survival of life on earth. The scarcity of clean water is a global issue that poses serious challenges to the survival of all living species (Zondo et al., 2022). The gas and oil industry is one of the biggest polluters of soil, air, surface, and groundwater (Costa et al., 2011). Oil exploration generates produced water that is characterized as hazardous and toxic waste and contains a mixture of dissolved and dispersed hydrocarbons which include benzene, toluene, ethylbenzene, and xylenes (commonly termed BTEX) (Dickhout et al., 2016; Fakhru'l-Razi et al., 2009). BTEX are listed as priority pollutants by the United States Environmental Protection Agency (USEPA) and are considered to be among the top 100 chemicals on the priority list of hazardous substances (USEPA, 2000). During the past several decades a number of remediation techniques have been explored for the sub-surface remediation of BTEX-contaminated soil and groundwater systems. These remediation techniques include physical (thermal treatment), biological (phytoremediation) and chemical (chemical oxidation) treatment (Khodaei et al., 2016). Among the various treatment methods used to treat produced water, and specifically for BTEX, membrane technologies using ultrafiltration (UF) processes are the leading method to remove these compounds. UF is classified as a low-pressure filtration process with a driving force applied from 100–1 000 kPa (Singh, 2005). UF membranes have pore sizes ranging from 0.1–0.01 μm and are capable of retaining molecules with a molecular range of 300 to 500 000 Da (Kulkarni et al., 1992). Polyethersulfone (PES) membranes offer advantages such as high efficiency, chemical and mechanical stability and low energy consumption, and are generally used in various separation processes (Singh, 2005). However, some limitations are accredited to their fairly hydrophobic surfaces which promote attachment of non-polar compounds on either membrane pores or membrane surfaces (Makhetha and Moutloali, 2020; Sadare et al., 2021).

In the past decade, reports on the application of tannic acid in membrane science to enhance surface chemistry have increased substantially (Fan et al., 2015; Pan et al., 2015; Kim et al. 2015; Fang et al., 2017; Yan et al., 2020). Tannic acid (TA) is a low-cost environmentally friendly natural polyphenol found in green tea, fruits, flowers and tree barks (Pan et al., 2015). Researchers have focused on utilizing hydroxyl groups from the TA galloyl group to react with each iron Fe^{III} to form a stable octahedral (Ross and Francis, 1978). Tannic acid and iron complex have been successfully used to modify the surfaces of the polymeric membrane by surface coating or blending, due to their abundant hydrophilic units on the surface of the tannic acid (Kim et al., 2015; Fan et al., 2015; Fang et al., 2017). Surface coating is the most commonly used method to modify membrane surfaces (Sadare et. Al., 2022). However, work conducted by Fang et al. (2017) proved effective in blending the TA-Fe^{III} complex within the polymer matrix. Blending is simple and different properties of the membrane can be achieved by differing the composition of the blend to obtain the desired membrane structure (Fang et al., 2017; Zahid et al., 2018). Fayemiwo et al. (2018) studied the adsorption removal

of BTEX compounds from water using a tannin-rich green tea gel adsorbent. The authors reported that green tea gel adsorbent showed great ability in adsorbing BTEX from water due to its hydroxyl (OH-) and carboxylic acid (C=O) groups. Several studies have investigated the removal of BTEX compounds in produced water using membrane technology. However, to the best of our knowledge, no studies have been conducted on the removal of BTEX compounds from produced water using tannins in membrane technology. The adsorption mechanism of tannin could be attributed to the combination of its highly porous structure and the presence of OH groups. In addition, it is hypothesized that the iron nanoparticles could adsorb pollutants because of their magnetic nature which permits them to aggregate for pore formation (Auffan et al., 2008). Therefore, in this work, the tannin iron complex (TA-Fe^{III}) complex was synthesized and incorporated within the polymer matrix as a hydrophilic additive to fabricate the TA-Fe^{III}/PES UF membrane. The fabricated membranes were characterized and evaluated for the removal of BTEX from water.

MATERIALS AND METHODS

Iron (III) chloride (FeCl$_3$) and tannic acid (TA) were purchased from Aladdin Shanghai (China). Polyethersulfone (PES M$_W$ =58 000 Da), analytical reagent N-methyl 2-pyrrolidinone 99.5% (NMP) was used as a solvent, benzene analytical grade (>99%) toluene analytical grade (99.5%), ethylbenzene analytical grade (>99.9%), xylene analytical grade (99.5%), methanol 99.995% HPLC grade and 99.5% acetone were purchased from Merck Co (South Africa). Naphthalene balls, C$_{10}$H$_8$, were purchased from Associated Chemical Enterprise (ACE, Johannesburg South Africa). Deionized water was used as a non-solvent in the coagulation bath. Each reagent was used as received without further treatment.

Membrane preparation

PES and PES modified membranes were fabricated using the non-solvent induced phase separation method (NIPS), as reported in the literature (Fang et al., 2017). Before commencing test work, 100 g PES beads were oven-dried at 80°C for 24 h to remove excess moisture. Casting solutions were prepared as described in Table 1. Casting solution of the pristine PES membrane was prepared in the following manner: PES (16 g) was completely dissolved by stirring in NMP (82 mL) at room temperature for 24 h. NMP solvent was selected as it is widely accepted as a good solvent for many polymers (Maximous et al., 2009). TA-Fe^{III}/PES membranes were prepared in the following manner: three (3) different loadings of TA/FeCl$_3$ (0.25/0.05 g), (0.5/0.1 g), (0.75/0.15 g) were dissolved in 20 mL NMP separately. To fabricate the mixed matrix membrane of various TA-Fe^{III} loadings, PES (16 g) was completely dissolved in residual NMP and then TA-Fe^{III} solutions with various loadings were dissolved in the PES solution under continuous mixing for 4 h at room temperature to ensure a casting solution which is homogeneous. Before being coated on a flat glass plate using SHEEN 1133N automated film applicator with a gap size of 250 μm, casting solutions were kept in an airtight bottle for 24 h to ensure that bubbles were not present in the solution.

Table 1. Composition of casting solution used to prepare the membranes

Membrane	PES (g)	TA-Fe^{III} (%)	NMP (mL)
PES-0	16	0.00	84.0
PES-0.3	16	0.30	83.0
PES-0.6	16	0.60	83.4
PES-0.9	16	0.90	83.1

The compositions of the casting solution used in the preparation of the membranes were chosen based on the study conducted by Fang et al. (2017).

Thereafter, the prepared membranes were immersed in a coagulation bath filled with deionized water after being exposed to the atmosphere for 30 s to allow partial evaporation of the solvent. For complete desorption of residual solvent, membranes were left in the bath for a minimum of 24 h.

Membrane characterization

In this study membrane morphology was analysed using surface and cross-sectional imaging by a field emission scanning electron microscope (FESEM, ZEISS GeminiSEM500 20kv). Surfaces of the membrane samples were coated with platinum to avoid charging, while for the cross-section membrane samples were first plunge-frozen in liquid nitrogen to enable freeze fracturing before coating with platinum. FTIR was conducted on attenuated total reflectance ATR-FTIR (spectrum 100, Perkin Elmer, USA) and used to identify the functional groups of the membrane. Spectra were collected over the range 400–4 000 cm^{-1}. Thermogravimetric analysis (TGA) was conducted on a TGA.STA 7200RV Hitachi with a heating rate of 10°C/min from 30°C to 900°C in nitrogen atmosphere with a purge rate of 20 mL/min. The contact angle of the membrane was measured using the sessile drop method (OCA 15 EC GOP, DATA Physics). Deionized water was used as a probe liquid and dispensed at 2 μL/s. Water droplets were placed on the membrane surface using a micro-syringe at 10 different positions (measured and averaged). Membrane surface roughness was measured using AFM Model Di 3000.

BTEX measurements

Internal standard (IS) methods are used to improve the precision and accuracy of results where volume errors are difficult to predict and control. An internal standard is a known concentration of compound present in every sample that is analysed. This is done to correct for the loss of analyte during sample preparation and sample inlet. A compound used as an internal standard should show similar behaviour (but not identical) to the analyte and has gas chromatograph retention time comparable to the analyte. It must be inert to the sample and must not react with the sample or the solvent used to dilute or prepare it. Naphthalene is a white, volatile solid polycyclic hydrocarbon with a strong mothball odour. Naphthalene chemical structure consists of two fused benzene rings and have physical properties suited to be used as a BTEX internal standard.

Compositional analysis

A standard solution of 2 μL of benzene, 2.1 μL of toluene, 2.1 μL ethylbenzene and 2.1 μL xylenes was dissolved into 10 mL of methanol to determine BTEX retention times. To prepare the IS, 0.01 g of naphthalene was dissolved in methanol to achieve a solution molarity of 0.225 mol/L. For every BTEX sample a known concentration of IS was injected to compare area peaks. A correction factor was included to account for any errors.

Chemical analysis of BTEX samples were conducted using Agilent Technologies 7820A GC system with flame ionization detector (GC–FID). RTX-200MS coated with cross bond trifluoropropyl methyl polysiloxane, 30 m long by 0.32 mm inner diameter (ID); 0.5 μm film thickness Agilent Technology carbon column was used in the gas chromatograph (GC). The GC–FID was operated in a 10:1 split mode and carrier gas was 99.999% nitrogen. The flame gas was a mixture of dry grade compressed air and nitrogen. To calibrate the GC, 1 μL of sample was directly injected into the column for analysis using a 10 μL micro syringe.

The column temperature was programmed as follows: isothermal temperatures in oven, injector and detector; oven temperature 50°C, hold time 5 min, ramp rate 15°C, maximum temperature 200°C; injector temperature 225°C; detector temperature 300°C.

Evaluation of fabricated membrane performance

Filtration performance of the membranes was assessed on a laboratory-scale dead-end filtration system consisting of a holding cell with a volume of 300 mL, an effective filtration area of 14.6 cm² and a maximum operating pressure of 1 000 kPa. The feed pressure was achieved by applying nitrogen gas. A fresh membrane was mounted onto the filtration cell and filled with deionised water. The membrane was compacted at a transmembrane pressure (TMP) of 150 kPa until a steady permeate was attained. To check the initial flux of the membrane, pressure was than lowered to 100 kPa to conduct pure water flux (PWF) experiments using Eq. 1. Each experimental run was accompanied by a new circular membrane sheet at room temperature (25±2°C) and the volume of the water permeate was collected after 10 min.

$$PWF = \frac{V}{At} \quad (1)$$

where PWF is pure water flux (L/(m²·h)), V (L) is volume of permeated water, A (m²) is the effective membrane area and t (h) is the permeation time.

After PWF experiments, the filtration cell was emptied and refilled with BTEX-contaminated water to conduct rejection studies. The ability of the membrane/s to remove specific BTEX pollutants from water was determined by rejection (%R). Rejection of the membranes was conducted using synthetic 70 mg/L BTEX solution. A volumetric flask measuring 1 L was filled with distilled water and the water was spiked with 70 mg/L of each compound to prepare synthetic BTEX wastewater. Membrane rejection was calculated by dividing the difference between the concentration of a specific pollutant in the feed (C_f) with the concentration of a specific pollutant in the permeate (C_p), as shown in Eq. 2. BTEX concentration in the feed and permeate solution was determined using Agilent 7820A GC–FID.

$$\left(\% R\right) = \left(1 - \frac{C_p}{C_f}\right) \times 100 \quad (2)$$

RESULTS AND DISCUSSION

Physicochemical characterization of fabricated membranes

Figure 1a depicts the surface morphology of the pristine membrane (PES 0) and Fig. 1b–d depicts the surface morphologies of the TA-Fe^{III} complex/PES membranes at different TA-Fe^{III} complex compositions of 0.3, 0.6 and 0.9 wt%, respectively. Top surface micrographs of all the membranes showed a typical UF membrane with a uniform porous structure. No noticeable changes were seen on the top surface of the membranes with the addition of hydrophilic additive TA-Fe^{III} complex. It should be noted that increasing the TA-Fe^{III} concentration in the casting solution increased viscosity of the casting solution, thus could have affected the surface pore size.

In addition to the surface morphology, energy dispersive X-ray (EDX) was used to confirm the presence of the TA-Fe nanoparticle composites in the membranes (Fig. 2). The presence of the Fe element was observed, confirming that the membranes contain TA-Fe^{III} nanoparticles. Besides the expected carbon, sulfur, and oxygen molecules found in a PES membrane, addition of TA-Fe^{III} complex loading showed an increase in iron molecules from PES-0.3 to PES-0.9. The increased energy intensity in line with increasing metal content in the formulation confirms that the systematic presence of TA-Fe^{III}, as expected, was observed.

Figure 3a–d depicts the cross-sectional views of the fabricated membranes at TA-Fe^{III} loading of 0, 0.3, 0.6 and 0.9 wt%, respectively. Membranes fabricated from PES are asymmetric in structure with a dense selective layer and finger-like macro-void sublayer (Goh et al., 2020). All the membranes fabricated produced the characteristic asymmetric structure found in polymeric membranes with a spongy inner surface. Results obtained from Fig. 2a showed that PES 0 had a thin top layer with a finger-like sublayer. During the immersion precipitation process, PES 0 experienced instantaneous de-mixing when the casting solution was immersed in the coagulation bath. This led to a quicker solvent–nonsolvent exchange rate, producing a porous top layer with finger-like sublayer (Mulder, 1991). Upon addition of TA-Fe^{III} complex on the PES membrane, PES 0.3 membrane experienced delayed de-mixing. Delayed de-mixing is a slow process in which de-mixing takes time and the solvent–nonsolvent exchange rate takes place at a slow rate after immersion in the coagulation bath (Fig. 2b). Hence, a dense top layer with a
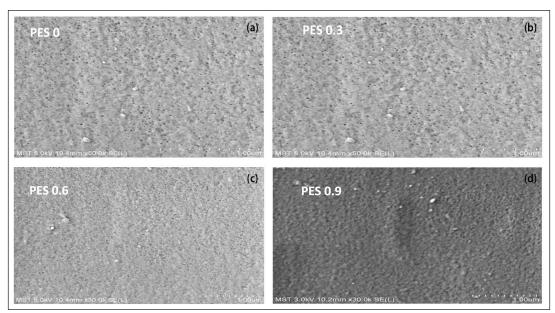

Figure 1. FE-SEM surface morphology of (a) PES 0, (b) PES 0.3, (c) PES 0.6 and (d) PES 0.9 blended membranes
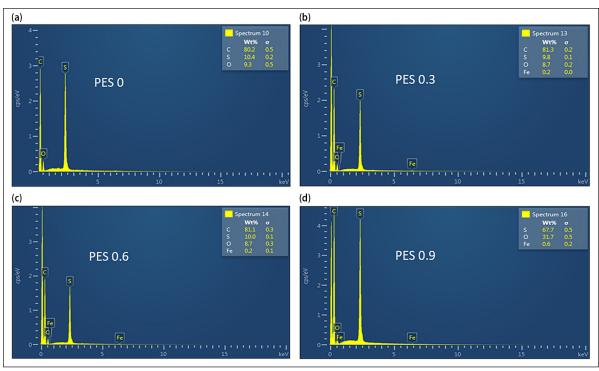
Figure 2. EDX results for different loadings of TA-Fe^{III} complex in the fabricated PES membranes
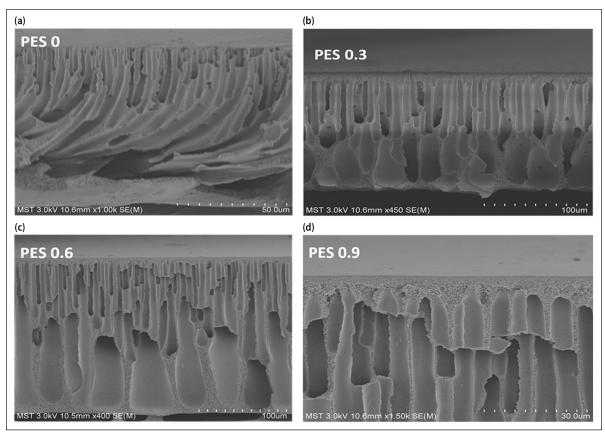

Figure 3. FE-SEM cross-sectional image of PES 0 to PES 0.9 blended membranes

narrowed channel, having few macrovoids in the sublayer, was observed when compared to PES 0 (Mulder, 1991).

Also, there is a visible change in the shape of the PES 0.3 macrovoids – the shape changed from a finger-like to pear-like structure when compared to PES 0. This change in the macrovoid structure was due to the increased polymer concentration when the TA-Fe^{III} was added. A pear-like structure refers to an increased porosity of the membrane due to a delay in mixing (Holda and Vankelecom, 2015). A dense top layer was observed for PES 0.3 when compared to PES 0. This happens during immersion precipitation when the solvent (NMP) displays a low affinity towards water in the coagulation bath. This causes

a low diffusion rate between solvent and nonsolvent leading to polymer concentration on the surface causing delayed mixing in the coagulation bath (Fahrina et al., 2018). PES 0.6 and PES 0.9 carried the same cross-sectional structure as PES 0.3, indicating that increasing the concentration of the TA-Fe^{III} complex from PES 0.6 to PES 0.9 does not change the morphology of the membrane further. From the cross-sectional images, it could be concluded that addition of the TA-Fe^{III} complex concentration affects the morphology of the membrane by expanding the channels and having broader internal pores. The results obtained in this study are comparable to literature (Fang et al., 2008).

Attenuated total reflectance–Fourier transform infrared (ATR–FTIR)

A pure PES structure contains an ether bond, benzene ring and a sulfone bond. FTIR spectra of the pure PES and TA-Fe^{III}/PES membrane are shown in Fig. 4. The peak at 1 240 and 1 242 cm^{-1} was assigned to the aromatic ether (Ar–O–Ar). The peaks at 1 305 and 1 152 cm^{-1} were assigned to the SO$_2$ bonds (S=O). The three aryl peak (C=C stretching) vibrations were observed between 1 400 and 1 600 cm^{1}. The C-H stretching peak of the benzene ring was observed at 2 975 and 3 086 cm^{-1}. The peaks from 3 000–3 500 cm^{-1} indicate the stretching of OH radicals. The above results were found to be similar to what other researchers have reported in literature (Makhetha and Moutloali, 2018; Aryanti et al., 2019). The vibration band found at 1 672 cm^{-1}, highlighted by a straight line, represents the C=O stretching band of NMP (Ponzio et al., 2001), indicating the presence of NMP. NMP solubilizes PES because it can interact strongly with the PES chains. Due to these strong interactions some solvent remained in the polymer during the phase inversion process and was not washed out properly, hence it appeared on the FTIR spectra. The decrease in intensity of the band when the TA-Fe^{III} membranes are fabricated is due to the NMP solvent washing out well. Less than 1% concentration of TA-Fe^{III} is added on the polymer matrix making it difficult to detect the TA molecule (C=O) in the FTIR spectra. Fe is a metal and its spectra are found below the fingerprint region; hence it could not be detected.

Thermogravimetric analysis (TGA)

Figure 5 illustrates the TGA profile of the pristine PES and TA-Fe^{III} complex/PES modified membranes. The first weight loss, <200°C, experienced by PES 0 could be attributed to evaporation of solvent (NMP boiling point is around 202°C) and water from the membrane while the TA-Fe^{III} modified membranes experienced weight loss from the evaporation of the solvent and water from condensation of the phenolic hydroxyl groups at 200°C (Xia et al., 2018). Tannic acid consists of a central core of glucose and two (inner and outer) layers of five gallic acids units. The five-outer layer of the five galloyl units starts decomposing above 350°C via decarboxylation (Nam et al., 2019, Xia et al., 2015). To completely incinerate the pure PES membrane, percentage weight loss should be directly proportional to the content of the PES (Fang et al., 2017). The increased weight loss for the modified membranes is confirmation of the presence of TA-Fe^{III} complex in the blend of membrane composition.
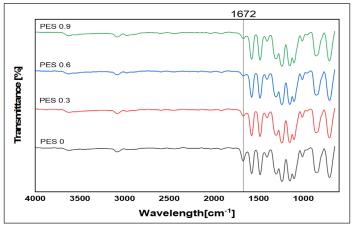

Figure 4. FTIR spectra of PES and PES blended membranes with various TA-Fe^{III} complex loading
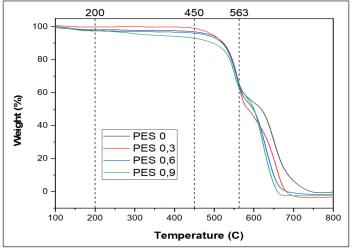

Figure 5. TGA analysis of PES and TA-Fe^{III} complex of various loadings

Membrane hydrophilicity (water contact angle)

The hydrophilicity of the fabricated membrane was evaluated by measuring the contact angle between the membrane surfaces and water droplets. Contact angle of membranes is considered to be an important parameter for membrane characterization and an indirect indication of the hydrophilicity and flux behavior (Abdallah et al., 2015; Ntshangase et al., 2021). As shown in Fig. 6, pure PES had a water contact angle of 75° corresponding to lower hydrophilicity. There is a subsequent drop in water contact angle as the iron tannin complex loading was increased, corresponding to increased surface hydrophilicity. Upon adding the TA-Fe[III] complex, the water contact angle of all the modified membranes decreased significantly. PES 0.3 had a water contact angel of 59°, PES 0.6 had 56° and PES 0.9 had 50°. Loading of the TA-Fe[III] complex improved the surface hydrophilicity of the membrane. This was due to the abundant phenolic hydroxyl groups (OH-) found in the tannic acid (Yan et al., 2020). According to literature, hydrophilic groups such as -OH, and -NH$_2$ are known for enhancing surface hydrophilicity (Purkait, 2018). Phenolic hydroxyl groups in the tannic acid interact with the membrane via hydrogen bonding thereby adsorbing water molecules (Yan et al., 2020). It was anticipated that increasing the TA-Fe[III] complex on the membrane would make the membrane absorb more water, thereby reducing the adsorption of pollutants on the membrane. This trend of the water contact angle was also observed by other researchers (Kim et al., 2018; Fang et al., 2018).

Measurement of the membrane roughness using atomic force microscopy (AFM)

Figure 7 shows the AFM images of the pure PES and the Ta-Fe[III] complex modified membranes. R_{ms} is the standard deviation of all the vertical distances within the enclosed area and R_a is the average roughness which indicates the mean roughness of the surface relative to the plane. Surface roughness is an important parameter in understanding the fouling tendency of the membrane during filtration (Hilal and Johnsson, 2012, Tansel, 2008). The AFM micrographs show an increasing trend in both the R_{ms} and R_a of the membranes as the TA-Fe[III] concentration increased.

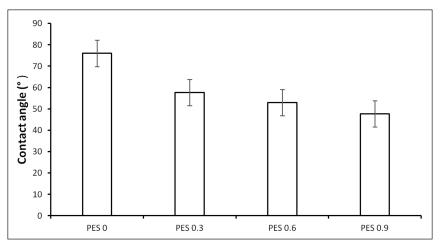**Figure 6.** Contact angle of PES and PES modified with various TA-Fe[III] complex loadings
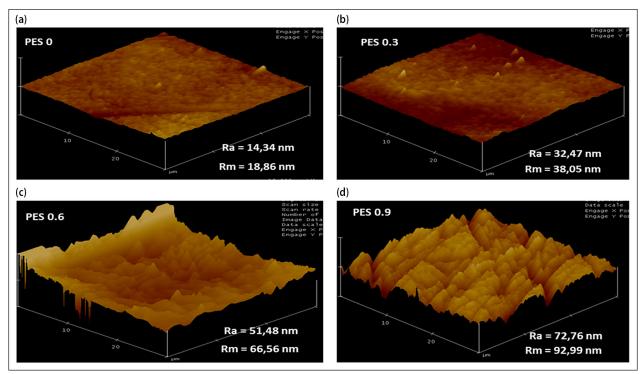

Figure 7. AFM images of (a) PES 0, (b) PES 0.3, (c) PES 0.6 and (d) PES 0.9 blended membranes evaluated at 2 x 2 μm scan area

PES O had small peaks on the surface but as TA-Fe^{III} is incorporated the valleys steadily increase and subsequently become large valleys. Small peaks represent smoothness while large valleys represent roughness. The roughness of the TA-Fe^{III}/PES membrane occurs when excess Fe^{III} induces aggregation of the TA-Fe^{III} complex on the membrane surface (Fan et al., 2015). Hydrophilic membranes with smooth membrane surfaces are less prone to fouling while rougher membranes promote attachment of foulants on the surface of the membrane, therefore increasing fouling rates (Singh, 2005; Dickhout et al., 2017; Makhetha and Moutloali, 2020). Based on these results these modified membranes are expected to foul quickly.

Performance evaluation of fabricated blended membranes

Membrane pure water flux (PWF)

Results for the pure water flux in Fig. 8 showed that as the TA-Fe^{III} loading increased the pure water flux also increased, thus supporting results obtained from the contact angle characterization. Pure water flux for PES 0 was initially 100 L/(m²·h), but upon addition of the TA-Fe^{III} complex, pure water flux improved significantly to 122 L/(m²·h) for PES 0.3, 130 L/(m²·h) for PES 0.6, and 150 L/(m²·h) for PES 0.9. Overall addition of the TA-Fe^{III} had a 50% increase in water flux compared to the pristine PES membrane. It is widely reported that improving surface hydrophilicity of membranes enhances water permeation by drawing water molecules inside the membrane matrix and advancing them to move more quickly through the membrane (Yan et al., 2020; Makhetha and Moutloali, 2018). Morphology of the membrane can also affect the performance of the membrane, especially the filtration process (Fahrina et al., 2018). Addition of the TA-Fe^{III} complex increased porosity and improved surface hydrophilicity thereby attracting additional water molecules to move more quickly throughout the membrane. These results are similar to those obtained for the contact angle, indicating that membranes with increased surface hydrophilicity have high pure water flux. In Fig. 3, micrographs show that the modified membranes exhibited expanded channels with increased porosity. Increased porosity reduced water resistance and provided extra routes for water to travel through the membrane.

Rejection of BTEX compounds

In membrane separation three main mechanisms are generally used: (i) size exclusion, (ii) hydrophobic interaction between pollutant and membrane and (iii) electrostatic interaction between the pollutant and the membrane (Kamali et al., 2019). The ability of the PES membrane and TA-Fe^{III}/PES composite membrane to separate BTEX compounds is shown in Fig. 9 and calculated as %R using Eq. 2. The BTEX compound concentrations were measured using a GC–FID. Upon receiving the results ethylbenzene and o-xylene colluded as one compound with the same retention time. Hence, in Fig. 8 they are reported as one compound, ethylbenzene + m-xylene.

Rejection by size exclusion was used to separate the BTEX compounds from water (Su et al., 2016; Aryanti et al., 2019). Results obtained for PES 0 showed the membrane had a rejection of 60% for benzene, 72% for toluene, 85% for ethylbenzene+m-xylene and 100% for xylene isomers (p;-o xylene). Rejection of ethylbenzene and xylenes was high due to the size of their compounds. When applying the 'membrane sieving principle' it was expected that competition between the individual compounds will occur for availability of the membrane pores. Since there is a limited number of pores on the surface of the membrane there will be competition between the BTEX compounds to permeate through the membrane pores. Benzene, being the smallest molecule in molecular weight and most soluble, will permeate through the available pores while the larger less-soluble compounds such as p- and o-xylenes will remain on the surface of the membrane or inside the pores and not permeate. These rejection results were similar to that reported by Su et al. (2016). They both achieved a rejection rate > 80%. However, the TA-Fe^{III}/PES membranes are much simpler to fabricate than the CNT/PDVF nanocomposite membranes.

BTEX solubility in water was in the order X < E < T < B. Upon increasing the concentration of TA-Fe^{III} complex to 0.3 wt%, rejection increased significantly to over 95% for the BTEX compounds. The high BTEX rejection was due to the membranes dense top and increased hydrophilicity with addition of the TA-Fe^{III} complex. When the concentration of TA-Fe^{III} complex was increased further to 0.6 wt% and 0.9 wt%, rejection of benzene and toluene decreased slightly; this was caused by poor selectivity of the membrane. The trade-off between permeability and selectivity can be attributed to the poor dispersion of TA-Fe^{III} on the membrane which caused the formation of agglomerates (Rameetse, 2020). Agglomeration results in increased macro-voids, hence allowing the soluble molecules, benzene and toluene, to pass through.

Table 2 presents the comparison of the results of this study with those reported in literature. A study conducted by Unuigbe et al. (2019) fabricated iron nanoparticles from pomegranate
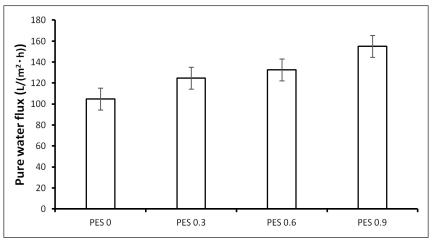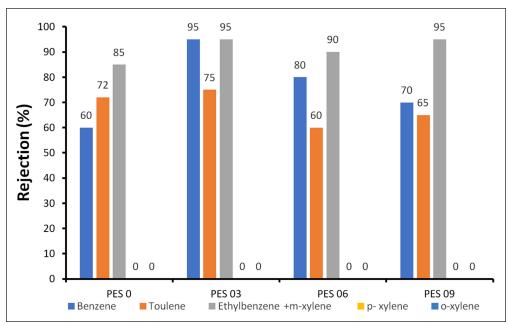

Figure 8. Effect of TA-Fe^{III} complex loading on the pure water flux (PWF). Experimental conditions: temperature = 25°C, pressure = 100 kPa, time = 10 min

Figure 9. Rejection of benzene, toluene, ethylbenzene and xylenes using PES 0 and PES modified with various TA-Fe^{III} complex loadings. Experimental conditions: temperature = 25°C, pressure = 100 kPa, time = 10 min

Table 2. Comparison of BTEX removal performance using membrane technology

Membrane	Permeate flux L/(m²·h)	Wastewater pollutant	%R	Ref
Fe-NP's/PES	80.05	BTEX	63.8	Unuigbe et al., 2019
Carbon nanotubes Polyvinylidene fluoride (CNT/PVDF) NF composite membrane	7	BTEX	80	Su et al., 2016
TA-Fe^{III}/PES	150	BTEX	93	This study

leaves and embedded them in PES membrane for the removal of BTEX compounds from water. The study reported good dispersion of the iron nanoparticle within the PES membrane and a maximum BTEX removal of 63% for the 10 wt% Fe-NPs at 100 kPa was attributed to the improved physico-chemical properties of the PES membrane due to the nanoparticles. Su et al. (2016) reported a rejection > 80% for BTEX on a CNT/PVDF nanocomposite membrane at ~70 kPa on crossflow filtration due to the outstanding properties of the carbon nanotubes (CNT). This study also performed well in removing BTEX from water as it had a rejection >80%. Membranes modified with TA-Fe^{III} complex had an enhanced PWF and anti-fouling properties due to the abundant hydrophilic (OH$^-$) units of the tannic acid, thereby increasing BTEX rejection.

CONCLUSION

The aim of the work was to fabricate TA-Fe^{III}/PES UF membrane via phase inversion and evaluate the performance of the membranes for the removal of BTEX compounds from water. Different characterization techniques were employed on the membrane and performance evaluation of the membrane was determined using dead-end filtration. Characterization results from the SEM, contact angle, and AFM showed that increasing the TA-Fe^{III} loading changed the membrane pore structure, increased hydrophilicity and made the membranes smoother. The fabricated TA-Fe^{III}/PES membrane showed enhanced permeability from 100 to ~150 L/(m²·h) for PES 0 and PES 0.9, respectively, at 100 kPa. In terms of rejection, the modified TA-Fe^{III}/PES membranes had a rejection percentage of >70% for benzene and toluene compared to the 60% rejection recorded for pure PES membrane. Rejection

of the BTEX compounds happened mainly through the size exclusion mechanism. The increased hydrophilicity and surface smoothness of the TA-Fe^{III}/PES membrane also improved the anti-fouling property of the membranes. Overall, PES 0.9 wt% was the best performing membrane in terms of hydrophilicity, PWF, rejection and antifouling property. Based on this study, these modified membranes proved to be effective in treating BTEX wastewater and do have potential to be applied in wastewater treatment. It is recommended that real BTEX wastewater from petrochemical sites be used to determine the true performance of the modified membranes.

AUTHOR CONTRIBUTIONS

Conceptualization – MOD, KM and RMM; writing, original draft preparation – TM, OS; writing, review and editing – OS, KM and MOD; visualization – MOD, OS, TM, and KM; acquisition of data via instrumentation – TM, SW; supervision – KM, MOD and RMM; project administration – KM. All authors have read and agreed to the published version of the manuscript.

FUNDING

ACKNOWLEDGEMENT

CONFLICT OF INTEREST

The authors declare no conflict of interest.

REFERENCES

ABDALLAH H, SHALABY MS and SHABAN AMH (2015) Performance and characterization for blend membranes of PES with manganese (III) acetylacetonate as metalorganic nanoparticles. *Int. J. Chem. Eng.* **1–2** 1–4. https://doi.org/10.1155/2015/896486

AUFFAN M, ROSE J, PROUX O, BORSCHNECK D, MASION A, CHAURAND P, HAZEMANN JL, CHANEAC C, JOLIVET JP, WIESNER MR and VAN GEEN A (2008) Enhanced adsorption of arsenic onto maghemite nanoparticles: As (III) as a probe of the surface structure and heterogeneity. *Langmuir.* **24** (7) 3215–3222. https://doi.org/10.1021/la702998x

ARYANTI N, KUSWORO TD, OKTIAWAN W and WARDHANI DH (2019) Performance of ultrafiltration- ozone combined system for produced water treatment. *Period. Polytechn. Chem. Eng.* **63** (3) 438–447. https://doi.org/10.3311/PPch.13491

COSTA AS, ROMAO LPC, ARAUJO BR, LUCAS SCO, MACIEL STA, WISNIEWSKI A and ALEXANDRE MR (2012) Environmental strategies to remove volatile aromatics fractions (BTEX) from petroleum industry wastewater using biomass. *Bioresour. Technol.* **105** 31–39. https://doi.org/10.1016/j.biortech.2011.11.096

DICKHOUT JM, MORENO J, BIESHEUVEL PM, BOELS L, LAMMERTINK RGH and DE VOS WM (2017) Produced water treatment by membranes: A review. *J. Colloid Interf. Sci.* **487** 523–534. https://doi.org/10.1016/j.jcis.2016.10.013

FAHRINA A, MAIMUN T, HUMAIR S, ROSNELLY CM, LUBIS MR, BAHRINA I, SUNARYA R, GHUFRAN A and ARAHMAN N (2018) The morphology and filtration performances of poly(ethersulfone) membrane fabricated from different polymer solution. *MATEC Web Conf.* **197** 09001. https://doi.org/10.1051/matecconf/201819709001

FAKHRU'L-RAZI A, PENDASHTEH A, ABDULLAH LC, BIAK DRA, MADAENI SS and ABIDIN ZZ (2009) Review of technologies for oil and gas produced water treatment. *J. Hazardous Mater.* **170** (2–3) 530–551. https://doi.org/10.1016/j.jhazmat.2009.05.044

FAN L, MA Y, SU Y, ZHANG R, LUI Y, ZHANG Q and JIANG Z (2015) Green coating by coordination of tannic acid and iron ions for antioxidant nanofiltration membranes. *R. Soc. Chem. Adv.* **5** (130) 107777–107784. https://doi.org/10.1039/C5RA23490E

FANG X, LI J, LI X, PAN S, SUN X, SHEN J, HAN W, WANG L and VAN DER BRUGGEN B (2017) Iron-tannin-framework complex modified PES ultrafiltration membranes with enhances filtration performance and fouling resistance. *J. Colloid Interface Sci.* **505** 642–652. https://doi.org/10.1016/j.jcis.2017.06.067

FAYEMIWO OM, DARAMOLA MO and MOOTHI K (2018) Tannin based adsorbents from green tea leaves for removal of monoaromatic hydrocarbon in water: Preliminary investigations. *Chem. Eng. Comm.* **205** (4) 549–556. https://doi.org/10.1080/00986445.2017.1409738

GOH PS, WONG WT, LIM JW, ISHMAIL AF and HILAL N (2020) Chapter 9 - Innovative and sustainable membrane technology for wastewater treatment and desalination application. *Innov. Strat. Environ. Sci.* **2020** 291–319. https://doi.org/10.1016/b978-0-12-817382-4.00009-5

HILAL N and JOHNSON D (2010) The use of atomic force microscopy in membrane characterization. *Comprehens. Membr. Sci. Eng.* **1** 337–354. https://doi.org/10.1016/B978-0-08-093250-7.00025-6

HOLDA AK and VANKELECOM IFJ (2015) Understanding and guiding the phase inversion process for synthesis of solvent resistant nanofiltration membranes. *J. Appl. Polymer Sci.* **132** (27) 1–17. https://doi.org/10.1002/app.42130

KHODAEI K, NASSERY HR, ASADI MM, MOHAMMADZADEH H and MAHMOODLU MG (2016) BTEX biodegradation in contaminated ground water using a novel strain (*Pseudomonas* sp. BTEX- 30). *Int. Biodeterior. Biodegrad.* **116** 234–242. https://doi.org/10.1016/j.ibiod.2016.11.001

KIM KY, KIM DG, KIM H, CHOI YS, YOON J and LEE JC (2015) Polyphenol/Fe[III] complex coated membranes having multifunctional properties prepared by a one-step fast assembly. *Adv. Mater. Interf.* **2** (14) 1500298. https://doi.org/10.1002/admi.201500298

KULKARNI SS, FUNK EW and LI NN (1992) Membrane handbook. In: Ho WSW and Sirkar KK (ed.) *Ultrafiltration: Introduction and Definition.* Van Nostrand Reinhold, New York. 387–393.

MAKHETHA TA and MOUTLOALI RM (2018) Antifouling properties of Cu(tpa)@GO/PES composite membranes and selective dye rejection. *J. Membr. Sci.* **554** 195–210. https://doi.org/10.1016/j.memsci.2018.03.003

MAKHETHA TA and MOUTLOALI RM (2020) Stable zeolitic imidazolate framework -8 supported onto graphene oxide hybrid ultrafiltration membranes with improved fouling resistance and water flux. *Chem. Eng. J. Adv.* **1** 1–13. https://doi.org/10.1016/j.ceja.2020.100005

MULDER M (1991) *Basic Principles Of Membrane Technology.* Kluwer Academic Publishers, Dordrecht. https://doi.org/10.1007/978-94-009-1766-8

NAM S, EASSON MW, CONDON BD, HILLYER MB, SUN L, XIA Z and NAGARAJAN R (2019) A reinforced thermal barrier coat of a Na-tannic acid complex from the view of thermal kinetics. *RSC Adv.* **9** 10914–10926. https://doi.org/10.1039/C9RA00763F

NGOBENI R, SADARE OO and DARAMOLA MO (2021) Synthesis and evaluation of HSOD/PSF and SSOD/PSF membranes for removal of phenol from industrial wastewater *Polymers.* **13** 1253. https://doi.org/10.3390/polym13081253

NTSHANGASE NC, SADARE OO and DARAMOLA MO (2021) Effect of silica sodalite functionalization and PVA coating on performance of sodalite infused PSF membrane during treatment of acid mine drainage. *Membranes.* **11** 315. https://doi.org/10.3390/membranes11050315

PADAKI M, MURALI RS, ABDULLAH MS, MISDANI N, MOSLEHYANI A and KASSIM MA (2015) Membrane technology enhancement in oil-water separation: A review. *Desalination.* **357** 197–207. https://doi.org/10.1016/j.desal.2014.11.023

PAN L, WANG H, WU C, LIAO C and LI L (2015) Tannic acid coated polypropylene membrane as a separator for lithium-ion batteries. *Appl. Mater. Interf.* **7** (29) 16003–16010. https://doi.org/10.1021/acsami.5b04245

PONZIO EA, ECHEVARRIA R, MORALES GM and BARBERO C (2001) Removal of N-methylpyrrolidone hydrogen-bonded to polyaniline free-standing films by protonation-deprotonation cycles or thermal heating. *Polymer Int.* **50** (11) 1180–1185. https://doi.org/10.1002/pi.755

PURKAIT MK, SINHA MK, MONDAL P and SINGH R (2018) Chapter 1 – Introduction to membranes, *Interf. Sci. Technol.* **25** 1–37. https://doi.org/10.1016/B978-0-12-813961-5.00001-2

RAMEETSE MS, ABEREFA O and DARAMOLA MO (2020) Effect of loading and functionalization of carbon nanotube on the performance of blended polysulfone/polyethersulfone membrane during treatment of wastewater containing phenol and benzene. *Membranes.* **10** 54. https://doi.org/10.3390/membranes10030054

ROSS TK and FRANCIS RA (1978) The treatment of rusted steel with mimosa tannin. *Corrosion Sci.* **18** (4) 351–361. https://doi.org/10.1016/S0010-938X(78)80049-3

SADARE OO, EJEKWU O, MOSHOKOA MF, JIMOH MO and DARAMOLA MO (2021) Membrane purification techniques for recovery of succinic acid obtained from fermentation broth during bioconversion of lignocellulosic biomass: current advances and future perspectives. *Sustainability.* **13** (12) 6794. https://doi.org/10.3390/su13126794

SADARE OO, YORO KO, MOOTHI K and DARAMOLA MO (2022) Lignocellulosic biomass-derived nanocellulose crystals as fillers in membranes for water and wastewater treatment: a review. *Membranes.* **12** 320. https://doi.org/10.3390/membranes12030320

SINGH R (2005) Chapter 1 – Introduction to membrane technology in hybrid membrane systems for water purification. In: Singh R (ed.) *Membrane Technology and Engineering for Water Purification* (2nd edn.). Elsevier. 80 pp. https://doi.org/10.1016/B978-0-444-63362-0.00001-X

SU F, LU C and TAI JH (2016) Separation of benzene, toluene, ethylbenzene and p-xylene from aqueous solution by carbon-nanotubes/polyvinylidene fluoride nanocomposite membrane. *J. Water Resour. Protect.* **8** 913–928. https://doi.org/10.4236/jwarp.2016.810075

TANSEL B (2008) Extracellular polymeric substances and membrane fouling: microtopographical characterization of fouling phenomena by atomic force microscopy. In: *Proceedings of the Water Environment Federation Membrane Technology Conference* [CD-ROM], 27–30 January 2008, Atlanta, GA. Water Environment Federation, Alexandria, VA. 432–437.

UNUIGBE CF, FAYEMIWO OM and DARAMOLA MO (2019) Synthesis and performance evaluation of iron nanoparticles polyethersulfone (Fe-NPs/PES) for BTEX removal from wastewater. *Water Environ. J.* **34** 74–86. https://doi.org/10.1111/wej.12506

USEPA (United States Environmental Protection Agency) (USEPA) (2000) *Innovative Remediation Technologies: Field Scale Demonstration Projects in North America* (2nd edn). EPA 542-B-00-004. USEPA, Washington DC.

XIA Z, SINGH A, KIRATITANAVIT W, MOSURKAL R, KUMAR J and NAGARAJAN R (2015) Unraveling the mechanism of thermal and thermo-oxidative degradation of tannic acid. *Thermochim. Acta.* **605** 77–85. https://doi.org/10.1016/j.tca.2015.02.016

XIA Z, KIRATITANAVIT W, FACENDOLA P, THOTA S, YU S, KUMAR J, MOSURKAL R and NAGARAJAN R (2018) Fire resistance polyphenols based on chemical modification of bio-derived tannic acid. *Polymer Degrad. Stability.* **153** 227–243. https://doi.org/10.1016/j.polymdegradstab.2018.04.020

YAN W, SHI M, DONG C, LIU L and GAO C (2020) Applications of tannic acid in membrane technologies: A review. *Adv. Colloid Interf. Sci.* **284** 1–23. https://doi.org/10.1016/j.cis.2020.102267

ZAHID M, RASHID A, AKRAM S, REHAN ZA and RAZZAQ W (2018) A comprehensive review on polymeric nano-composite membranes for water treatment. *J. Membr. Sci. Technol.* **8** (1) 1–20. https://doi.org/10.4172/2155-9589.1000179

ZONDO BZ, SADARE OO, SIMATE GS and MOOTHI K (2022) Removal of Pb^{2+} ions from synthetic wastewater using functionalized multi-walled carbon nanotubes decorated with green synthesized iron-gold nanocomposites. *Water SA.* **48** (3) 304–316. https://doi.org/10.17159/wsa/2022.v48.i3.3959